Axial Strength Model for FRP Confined Concrete-Filled Steel Tube Columns

Abdullah[1*], *Hasnain Ali* [2], *Fahad Aslam* [3], *Mehar Ali*[4] and *Ali Raza*[5]

[1,2,3,4,5]Department of Civil Engineering, University of Engineering and Technology Taxila, 47050, Pakistan abdullahtts408@gmail.com, hasnainali1749@gmail.com, aslamfahad113@gmail.com, meharaliali25@gmail.com, ali.raza@uettaxila.edu.pk

Abstract: Numerous studies have delved into anticipating the load-carrying capacity (LC) of fiber-reinforced polymer (FRP)-confined concrete-filled steel tubes (CFST) compression members (SFC) using limited and noisy data. However, none have undertaken a comparative assessment of the accuracy among various modeling techniques based on an extensive and refined database. This study aims to introduce an analytical model for forecasting the LC of SFC compression members. The model is developed utilizing a database comprising 712 samples, considering the mechanism of confinement of both tubes of steel and FRP wraps. By incorporating the lateral confinement mechanism of SFC columns, the analytical model yields precise predictions. As per the experimental database, the analytical model demonstrates statistics such as MAE = 427, MAPE = 283, R2 = 0.815, RMSE = 275, and an a20-index = 0.73, indicating its effectiveness in providing accurate predictions.

Keywords: Database, Fiber reinforced polymers; concrete-filled steel tube; analytical model

1 Introduction

The concrete compression members when fiber-reinforced confined polymers (FRP) and steel tubes (ST) present a remarkable mechanical performance and smartness. These members are widely recommended in civil engineering projects such as long-span bridges and multistory buildings [1-4]. In contrast to carbon steel, stainless steel in concrete production is generally preferred due to numerous characteristics including but not limited to high durability, high-temperature resistance, improved mechanical characteristics, aesthetic appeal, minimal cost of maintenance, and strong tolerance to corrosive environment [5, 6]. Stainless ST offers better axial compressive strength to concrete compression members with external confinement. Nonetheless, after the possible buckling of these members, the efficacy of ST is comprised of the ultimate reduction in associated load-bearing capacity and ductility of compression members [7, 8]. To address these problems, FRP sheets are recommended to prevent the lateral buckling with an extra lateral confinement which in turn improves the axial stiffness of the ST [9]. With better confinement impact on concrete compression members, both ductility as well as axial compression strength are considerably enhanced which in turn improves their seismic performance [10-12].

Previously, several experimental studies have been carried out to assess the axial compressive performance of conventional ST and/or stainless-ST compression members subjected to

* Corresponding author : abdullahtts408@gmail.com

confinement with and without FRP wraps [13-16]. These studies revealed a considerable improvement in axial strain and strength of concrete compression members with better confinement impact from a combination of FRP and ST which eventually improves the core resistance against lateral buckling. Thereby, it portrays a considerable increase in load-bearing strength as well as ductility of compression members. Resulting modification in the characteristics of confined concrete microstructure would eventually impact both the confined concrete stress and splitting cracking in core concrete, which shows the interdependency between confining stresses and strains [17-19]. Nonetheless, the estimates obtained from analytical modeling are not accurate enough to capture the complexity of numerous parameters of FRP-confined concrete compression members due to noisy results with a limiting dataset. Thus, to get accurate estimates from analytical models, a large experimental database is required which involves a variety of FRP-confined sample variables.

Upon a comprehensive review of the literature, it is evident that previously established analytical models for capturing the load-bearing strength of SFC compression members were developed based on limited data points and curve-fitting procedures, which could compromise accuracy when dealing with noisy data. Furthermore, these models did not encompass all variables pertinent to SFC compression members, leading to inadequate estimation of the interaction mechanism between concrete compression members and confining surfaces. Existing analytical models for predicting the load-carrying capacity (LC) of concrete-filled steel tube (CFST) compression members confined with fiber-reinforced polymer (FRP) were limited by constrained experimental data and insufficient consideration of FRP confinement-related variables. These models failed to adequately address factors like the interaction between FRP wraps, steel tubes (ST), and concrete. Consequently, the development of a more inclusive model capable of precisely forecasting the load-bearing capacity of FRP-confined CFST compression members requires extensive research.

This study addresses this need by examining a broad range of factors related to FRP and steel tube confinement, drawing on a sizable database of 325 samples. Unlike experimental tests, analytical simulations require fewer computational resources while accounting for all the variables involved in the concrete confining mechanism. The performance of SFC compression members was assessed by the authors through the use of analytical modeling based on regression analysis and the experimental database. Using a database of 712 FRP-confined samples and taking into account all the confining mechanisms of steel and FRP tubes, an analytical model was created to estimate the LC of SFC compression members. To substantiate the current model's superiority over earlier literature research, a comparison of all previous models' predictions was carried out.

2 ANALYTICAL MODELING

2.1 Database

A detailed review of literature indicates that limited research on evaluating the LC of SFC compression members with analytical models. However, these models were limited by a small experimental database [20] and did not comprehensively account for the confining mechanism. In contrast, this study introduces a novel analytical model using two distinct

experimental databases, comprising 712 and 325 samples, respectively, for FRP-confined concrete and SFC columns. The databases were constructed by incorporating information from previously published investigations and updated to eliminate any noisy datasets that could introduce errors of more than 20% from the best-fit curves. The statistical data for the FRP-confined samples with 712 points are detailed in Table 1, including parameters such as the diameter of sample (D), height of the sample (L), thickness of FRP sheet (nt), elastic modulus of the sheet (E_f), unconfined concrete strength (f_{co}'), confined concrete strength (f_{cc}'), unconfined concrete strain (ε_{co}'), and confined concrete strain (ε_{cc}').

Table 1: Database statistics for FRP-confined columns

Parameter	D (mm)	L (mm)	nt (mm)	E_f GPa	f'_{co} (MPa)	f'_{cc} (MPa)	ε'_{co} (%)	ε'_{cc} (%)
Maximum	51	102	0.09	10	12.41	18.5	0.1676	0.083
Minimum	406	812	5.9	663	188.2	302.2	1.53	4.62
Average	153.37	306.94	0.88	172.03	41.97	75.58	0.27	1.52
St. Dev.	42.99	85.99	1.04	119.61	22.47	35.17	0.14	0.86
COV	0.29	0.29	1.19	0.7	0.54	0.47	0.52	0.57

The SFC columns database comprises parameters such as column area (A), height (H), steel tube thickness (t_{st}), yield strength (f_{st}), ultimate strain (ε_{st}), FRP ultimate strength (f_f), FRP tensile elastic modulus (E_f), FRP ultimate strain (ε_f), FRP sheet thickness (t_f), and column axial capacity (P_n). Statistical details for the developed database, containing 325 points, are presented in Table 2.

Table 2: Statistical details of the database for SFC columns

Parameter	A (mm^2)	H (mm)	fc' (MPa)	t_{st} (mm)	f_{st} (MPa)	ε_{st} (%)	f_f (MPa)	E_f (GPa)	ε_f (%)	t_f (mm)	P_n (kN)
Max.	125600	2000	140	8.8	729	5	4598	273	4.56	30	9358
Min.	7200	300	28	0.67	1.23	0.01	250	13.9	0.01	0	478
Avg.	21700	488	48.37	4.29	329	0.48	3076	184.1	0.75	1.28	2154
St. Dev.	21310	293	27.13	1.96	150	1.12	1156	86.14	0.9	2.81	1742
COV	0.98	0.6	0.56	0.46	0.46	2.33	0.38	0.47	1.2	2.2	0.81

2.2 Assessment of Previous Models

A few of the previously utilized analytical models [21-26] to assess the confined concrete samples' accuracy and generic form, an investigation was conducted using the created database. The strength of concrete confined within the steel tube (ST) is notably affected by the stress-path confining material. A distinct lag between the confining strain and axial strain and stress is evident, especially when stiffer concrete, as opposed to normal-strength concrete, experiences diminished crack propagation across different concrete strengths [27-29]. Simulating the load-carrying capacity (LC) of SFC compression members requires considering the core concrete compression strength with CFRP wrap confinement (P_{cc}) utilizing an established database. Additionally, the contribution of the external confining mechanism provided by the steel tube (ST) is determined for LC (P_{st}) using analytical

expressions. The analytical models adopted for assessing the LC of CCFRP-confined concrete incorporate these considerations [21-26] were examined over the developed database. Ultimately, this approach leads to an enhanced model, incorporating statistical parameters such as mean absolute error (MAE), determination coefficient (R^2), root mean squared error (RMSE), and a20-index, derived from equations (1-5), respectively. Here n indicates total number of samples, x_i designates the experimental results whereas y_i labels the estimated results.

$$MAE = \frac{1}{n}\sum_{i=1}^{n}|x_i - y_i| \tag{1}$$

$$R^2 = \left(\frac{n(\sum_{i=1}^{n} x_i y_i) - (\sum_{i=1}^{n} x_i)(\sum_{i=1}^{n} y_i)}{\sqrt{\left[n\sum_{i=1}^{n} {x_i}^2 - (\sum_{i=1}^{n} x_i)^2\right]\left[n\sum_{i=1}^{n} {y_i}^2 - (\sum_{i=1}^{n} y_i)^2\right]}}\right)^2 \tag{2}$$

$$MAPE = \frac{1}{n}\sum_{i=1}^{n}\left|\frac{x_i - y_i}{x_i}\right| \tag{3}$$

$$RMSE = \sqrt{\frac{1}{n}\sum_{i=1}^{n}(x_i - y_i)^2} \tag{4}$$

$$a_{20} - index = \frac{N_{20}}{n} \tag{5}$$

The symbol N_20 denotes the number of samples where the ratio of "experimental value" to "predicted value" falls within the 0.80 to 1.20 range. An ideal predictive model would result in an a20-index of 1. This proposed a20-index offers a practical engineering interpretation, indicating the percentage of samples where predicted values deviate by ±20% from the experimental values.

In contrast, Lam and Teng's strength model [30] outperformed other models, achieving R2 = 0.903 and RMSE = 0.244 across the experimental dataset. Consequently, this model was selected for curve fitting and regression analysis to ensure optimal predictions for the load-carrying capacity (LC) of SFC compression members. Figure 1 reports the assessment.

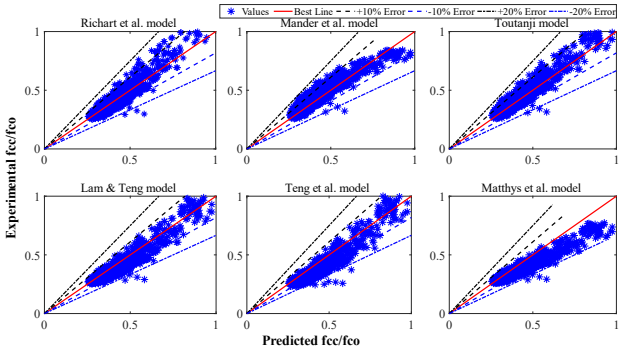

Figure 1: Evaluation of performance of various models.

2.3 Proposed Model

The load-carrying capacity (P_n) of SFC compression members is obtained by adding the axial compressive strength of the core concrete confined by CFRP (P_{cc}) with the axial compression strength contributed by the external confinement of the ST (P_{st}).

$$P_n = P_{cc} + P_{st} \tag{6}$$

The compressive strength of the core concrete subjected to confinement by CFRP sheets can be characterized as $P_{cc} = A_{cc} f'_{cc}$, Where, A_{cc} represents the area of the core concrete confined by CFRP layers, and f_{cc}' denotes the compression strength of the concrete core. Eq. (6) outlines the structure of the newly developed model for the axial compression strength of the core concrete with CFRP wraps.

$$f'_{cc} = f'_{co} + k f'^{1-n}_{co} f_l^{\,n} \tag{7}$$

Here f_l represents the ultimate confinement stress as proved to the concrete by CFRP wraps. Employing MATLAB to tackle statistical considerations (MAE and RMSE) and optimize the best-fit curve (R^2) across the dataset, the constants k and n were fine-tuned. The regression analysis outcomes revealed values of 3.1 for k and 0.83 for n. Eq. (7) outlines the conclusive expression for the axial compression strength of the core concrete under CFRP confinement.

$$f'_{cc} = f'_{co} + 3.1 f'^{0.22}_{co} f_l^{\,0.83} \tag{8}$$

Figure 2 reports the performance of this model having RMSE = 0.18 and R^2 = 0.94 over the developed experimental dataset. These parameters indicate better results obtained from this model than those of the previously used models.

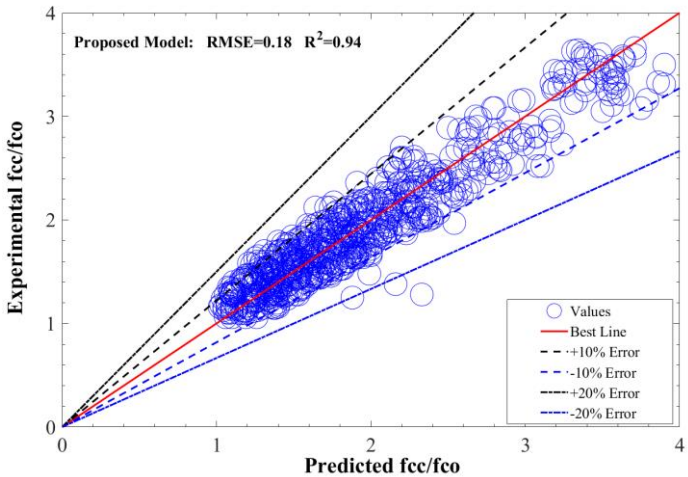

Figure 2: Evaluating the performance of the proposed strength model for the compression strength of FRP-confined concrete (f_{cc}').

Hence, to better understand the behavior of axial compression strength of core concrete under CFRP wraps (P_{cc}) Eq. (9) can be referred :

$$P_{cc} = A_{cc}\left[f'_{co} + 3.1 f'^{0.22}_{co} f_l^{\,0.83}\right] \tag{9}$$

Likewise, to evaluate the axial compression strength with the external confining mechanism from the ST (P_{st}) Eq. (10) can be used which acknowledges both the strain hardening as well as the resistances of ST subjected to the axial shortening by adopting the continuous strength approach [20, 31, 32].

$$P_{st} = A_{st}\sigma_{LB} \tag{10}$$

Within this equation, A_{st} represents the cross-sectional area of the steel tube, and σ_{LB} signifies the stress elucidating the localized buckling action of the tube. The strain hardening attributes of the steel tube play a pivotal role in influencing the load-carrying capacity (LC) and ductility of SFC compression members [33]. The parameter σ_{LB} can be derived using the following expressions [32] :

$$\sigma_{LB} = E\varepsilon_{LB}\frac{\varepsilon_{LB}}{\varepsilon_{0.2}} < 1.0 \tag{11}$$

$$\sigma_{LB} = \varepsilon_{0.2} + E_{sh}\varepsilon_{0.2}\left(\frac{\varepsilon_{LB}}{\varepsilon_{0.2}} - 1\right)\frac{\varepsilon_{LB}}{\varepsilon_{0.2}} \geq 1.0 \tag{12}$$

In this equation, ε_{LB} defines the local buckling action, E depicts the elasticity and $\varepsilon_{0.2}$ represents the 2% strain of the tube. Similarly, E_{sh} explains the elasticity of ST observed while the biaxial strain hardening process is executed. Buchanan and Gardner [32] followed a model to develop the association of deformation capacity (λ_c) with the cross-sectional slenderness of the tube and is expressed by Eq. (13).

$$\frac{\varepsilon_{LB}}{\varepsilon_{0.2}} = \frac{4.44 \times 10^{-3}}{\lambda_c^{4.5}} \leq minimum\left(15, \frac{0.1\varepsilon_u}{\varepsilon_{0.2}}\right) \tag{13}$$

Here, ε_u defines the highest strain of the ST. To conclude, the established model for the LC of SFC compression members can be described by Eq. (14) which explicitly considers the axial impact of ST, CFRP wraps, and their confining actions.

$$P_n = A_{cc}f'_{cc} + A_{st}\sigma_{LB} = A_{cc}\left[f'_{co} + 3.1{f'_{co}}^{0.22}{f_l}^{0.83}\right] + A_{st}\sigma_{LB} \tag{14}$$

The analytical model proposed for predicting the load-carrying capacity (LC) of SFC columns yielded the following statistics based on the experimental database of 325 SFC compression members: an a20-index of 0.73, an RMSE of 275, an MAE of 427, R2 of 0.815, and a MAPE of 283. Figure 3 illustrates the predictions of the proposed analytical model (Eq. 14) for the LC of SFC compression members.

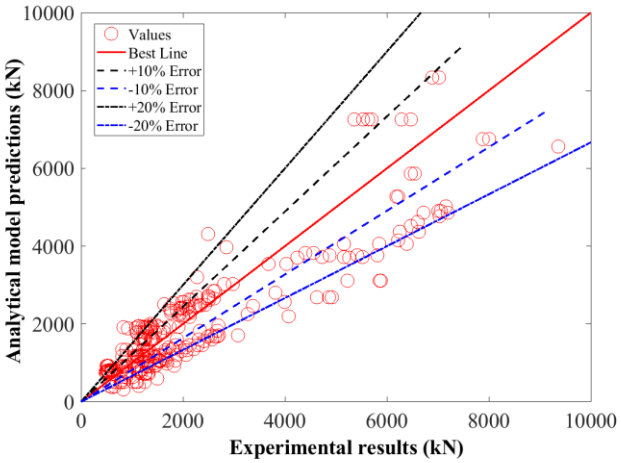

Figure 3: Predictions for the proposed model for LC of SFC columns.

3 Conclusions

This study employs a comprehensive analytical modeling approach supported by regression analysis and curve fitting to estimate the Load-Carrying (LC) capacity of fiber-reinforced polymer (FRP)-confined structural tube (ST) concrete-filled (SFC) compression members. The analysis is based on a substantial experimental dataset comprising 325 samples. The currently employed analytical model for the LC of SFC columns aligns well with experimental results, achieving an a20-index of 0.73, an RMSE of 275, an MAE of 427, and a MAPE of 283. This evaluation is grounded in confinement mechanics and various CFRP-confined strength models previously applied to a developed experimental database consisting of 712 members. In comparison to previously utilized models, the employed analytical model demonstrates superior accuracy by explicitly considering the restricting action of both CFRP wraps and ST.

References

1. Han, L.-H., W. Li, and R. Bjorhovde, Developments and advanced applications of concrete-filled steel tubular (CFST) structures: Members. Journal of constructional steel research, 2014. **100**: p. 211-228.
2. Raza, A., et al., Rapid repair of geopolymer concrete members reinforced with polymer composites: Parametric 00study and analytical modeling. Engineering Structures, 2024. **299**: p. 117143.
3. Zhang, B., et al., Seismic behaviour of FRP-concrete-steel double-tube columns with shear studs: Experimental study and numerical modelling. Engineering Structures, 2024. **302**: p. 117339.
4. Zhang, B., et al., Elliptical concrete-filled FRP tubes with an embedded H-shaped steel under axial compression and cyclic lateral loading: Experimental study and modelling. Composite Structures, 2024. **330**: p. 117839.
5. Al-Mekhlafi, G.M., M.A. Al-Osta, and A.M. Sharif, Behavior of eccentrically loaded concrete-filled stainless steel tubular stub columns confined by CFRP composites. Engineering Structures, 2020. **205**: p. 110113.
6. He, A., et al., Experimental and numerical investigations of circular recycled aggregate concrete-filled stainless steel tube columns. Journal of Constructional Steel Research, 2021. **179**: p. 106566.
7. Fam, A., F.S. Qie, and S. Rizkalla, Concrete-filled steel tubes subjected to axial compression and lateral cyclic loads. Journal of Structural Engineering, 2004. **130**(4): p. 631-640.
8. O'Shea, M.D. and R.Q. Bridge, Design of circular thin-walled concrete filled steel tubes. Journal of Structural Engineering, 2000. **126**(11): p. 1295-1303.
9. Cao, S., C. Wu, and W. Wang, Behavior of FRP confined UHPFRC-filled steel tube columns under axial compressive loading. Journal of Building Engineering, 2020. **32**: p. 101511.
10. Teng, J., et al., Three-dimensional finite element analysis of reinforced concrete columns with FRP and/or steel confinement. Engineering Structures, 2015. **97**: p. 15-28.

11. Zeng, L., et al., Experimental study of seismic performance of full-scale basalt FRP-recycled aggregate concrete-steel tubular columns. Thin-Walled Structures, 2020. **151**: p. 106185.
12. Cai, J., et al., Behavior of geopolymeric recycled aggregate concrete-filled FRP tube (GRACFFT) columns under lateral cyclic loading. Engineering Structures, 2020. **222**: p. 111047.
13. Asteris, P.G., et al., Evaluation of the ultimate eccentric load of rectangular CFSTs using advanced neural network modeling. Engineering Structures, 2021. **248**: p. 113297.
14. Memarzadeh, A., H. Sabetifar, and M. Nematzadeh, A comprehensive and reliable investigation of axial capacity of Sy-CFST columns using machine learning-based models. Engineering Structures, 2023. **284**: p. 115956.
15. Prabhu, G.G., M. Sundarraja, and Y.Y. Kim, Compressive behavior of circular CFST columns externally reinforced using CFRp composites. Thin-Walled Structures, 2015. **87**: p. 139-148.
16. Zhou, X., Z. Zhou, and D. Gan, Analysis and design of axially loaded square CFST columns with diagonal ribs. Journal of Constructional Steel Research, 2020. **167**: p. 105848.
17. Dong, C., A. Kwan, and J. Ho, A constitutive model for predicting the lateral strain of confined concrete. Engineering Structures, 2015. **91**: p. 155-166.
18. Kwan, A., C. Dong, and J. Ho, Axial and lateral stress–strain model for FRP confined concrete. Engineering Structures, 2015. **99**: p. 285-295.
19. Lai, M., L. Hanzic, and J.C. Ho, Fillers to improve passing ability of concrete. Structural Concrete, 2019. **20**(1): p. 185-197.
20. Sharif, A.M., G.M. Al-Mekhlafi, and M.A. Al-Osta, Structural performance of CFRP-strengthened concrete-filled stainless steel tubular short columns. Engineering Structures, 2019. **183**: p. 94-109.
21. Mander, J.B., M.J. Priestley, and R. Park, Theoretical stress-strain model for confined concrete. Journal of structural engineering, 1988. **114**(8): p. 1804-1826.
22. Lam, L. and J.G. Teng, Design-oriented stress–strain model for FRP-confined concrete. Construction and building materials, 2003. **17**(6-7): p. 471-489.
23. Toutanji, H., Stress-strain characteristics of concrete columns externally confined with advanced fiber composite sheets. Materials Journal, 1999. **96**(3): p. 397-404.
24. Teng, J., et al., Refinement of a design-oriented stress–strain model for FRP-confined concrete. Journal of composites for construction, 2009. **13**(4): p. 269-278.
25. Richart, F., A. Brandtzaeg, and R. Brown, The failure of plain and spirally reinforced concrete in compression. Bulletin 190. University of Illinois Engineering Experimental Station, Illinois, 1929.
26. Matthys, S., et al., Axial load behavior of large-scale columns confined with fiber-reinforced polymer composites. ACI Structural Journal, 2005. **102**(2): p. 258.
27. Lai, M., et al., A stress-path dependent stress-strain model for FRP-confined concrete. Engineering Structures, 2020. **203**: p. 109824.
28. Lai, M., et al., A path dependent stress-strain model for concrete-filled-steel-tube column. Engineering Structures, 2020. **211**: p. 110312.

29. Ho, J., et al., A path dependent constitutive model for CFFT column. Engineering Structures, 2020. **210**: p. 110367.
30. Lam, L. and J. Teng, Design-oriented stress–strain model for FRP-confined concrete. Construction Building Materials, 2003. **17**(6-7): p. 471-489.
31. Zhao O, A.S., Gardner L, Structural response and continuous strength method design of slender stainless steel cross-sections. Engineering Structures, 2017. **140**: p. 14-25.
32. Buchanan C, G.L., Liew A, The continuous strength method for the design of circular hollow sections. Journal of Constructional Steel Research, 2016. **118**: p. 207-16.
33. Tao, Z., et al., Nonlinear analysis of concrete-filled square stainless steel stub columns under axial compression. Journal of Constructional Steel Research, 2011. **67**(11): p. 1719-1732.